

An actively vetoed Clover γ -detector for nuclear astrophysics at LUNA

T. Szücs^{1,2}, D. Bemmerer^{3a}, C. Brogini⁴, A. Cacioli^{4,5}, F. Confortola⁶, P. Corvisiero⁶, Z. Elekes¹, A. Formicola⁷, Zs. Fülöp¹, G. Gervino⁸, A. Guglielmetti⁹, C. Gustavino⁷, Gy. Gyürky¹, G. Imbriani^{10,11}, M. Junker⁷, A. Lemut^{6b}, M. Marta³, C. Mazzocchi⁹, R. Menegazzo⁴, P. Prati⁶, V. Roca^{10,11}, C. Rolfs¹², C. Rossi Alvarez⁴, E. Somorjai¹, O. Straniero^{11,13}, F. Strieder¹², F. Terrasi^{11,14}, and H.P. Trautvetter¹²
(LUNA collaboration)

¹ Institute of Nuclear Research (ATOMKI), Debrecen, Hungary

² University of Debrecen, Debrecen, Hungary

³ Forschungszentrum Dresden-Rossendorf (FZD), Dresden, Germany

⁴ INFN Sezione di Padova, Padova, Italy

⁵ Dipartimento di Fisica, Università di Padova, Padova, Italy

⁶ Dipartimento di Fisica, Università di Genova, and INFN Sezione di Genova, Genova, Italy

⁷ INFN, Laboratori Nazionali del Gran Sasso, Assergi, Italy

⁸ Dipartimento di Fisica Sperimentale, Università di Torino, and INFN Sezione di Torino, Torino, Italy

⁹ Università degli Studi di Milano, and INFN Sezione di Milano, Milano, Italy

¹⁰ Dipartimento di Scienze Fisiche, Università di Napoli "Federico II", and INFN Sezione di Napoli, Napoli, Italy

¹¹ INFN Sezione di Napoli, Napoli, Italy

¹² Institut für Experimentalphysik III, Ruhr-Universität Bochum, Bochum, Germany

¹³ Osservatorio Astronomico di Collurania, Teramo, Italy

¹⁴ Seconda Università di Napoli, Caserta, Italy

Version accepted by Eur.Phys.J. A, March 26, 2021

Abstract. An escape-suppressed, composite high-purity germanium detector of the Clover type has been installed at the Laboratory for Underground Nuclear Astrophysics (LUNA) facility, deep underground in the Gran Sasso Laboratory, Italy. The laboratory γ -ray background of the Clover detector has been studied underground at LUNA and, for comparison, also in an overground laboratory. Spectra have been recorded both for the single segments and for the virtual detector formed by online addition of all four segments. The effect of the escape-suppression shield has been studied as well. Despite their generally higher intrinsic background, escape-suppressed detectors are found to be well suited for underground nuclear astrophysics studies. As an example for the advantage of using a composite detector deep underground, the weak ground state branching of the $E_p = 223$ keV resonance in the $^{24}\text{Mg}(p,\gamma)^{25}\text{Al}$ reaction is determined with improved precision.

PACS. 25.40.Lw Radiative capture – 29.30.Kv X- and gamma-ray spectroscopy – 29.40.Wk Solid-state detectors – 26.20.Cd Stellar hydrogen burning

1 Introduction

Recent advances in observations [1, e.g.] and in modeling [2,3] of the Sun and of stars have heightened the need for precise nuclear data on reactions of astrophysical interest. One approach to provide such data is to place a high-intensity particle accelerator deep underground, where the laboratory background in γ -ray detectors is reduced so that radiative capture reactions can be studied with improved sensitivity.

The Laboratory for Underground Nuclear Astrophysics (LUNA) has implemented this strategy, first with a 50 kV accelerator [4] and now with a 400 kV accelerator [5] placed in the underground facility of Laboratori Nazionali del Gran Sasso (LNGS)¹ in Assergi, Italy. LNGS is shielded from cosmic rays by a rock overburden equivalent to 3800 m water.

Benefiting from the resulting low γ -ray background, several nuclear reactions of astrophysical importance have been studied in recent years at LUNA [6,7,8,9,10,11,12,13]. In many cases, cross sections lower than ever reached before have been measured. Motivated by these advances,

^a e-mail: d.bemmerer@fzd.de

^b Present address: Lawrence Berkeley National Laboratory, Berkeley, USA

¹ Web site of the laboratory: <http://www.lngs.infn.it>

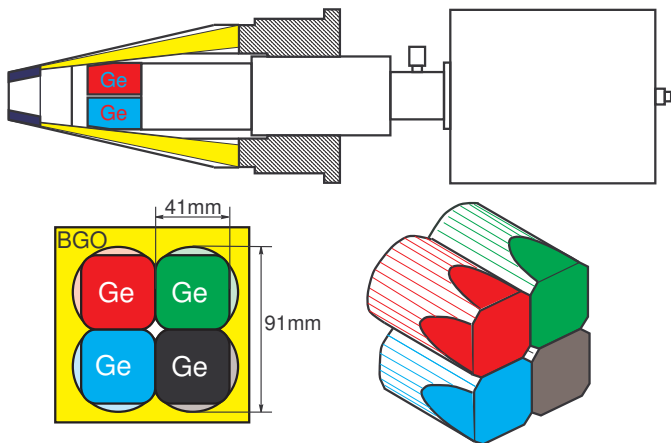


Fig. 1. Schematic cross section of the Clover-BGO system. The four germanium crystals are called red, green, black, and blue. The BGO escape-suppression shield (yellow) and the heavy-metal collimator on the front face (dark-blue) are also shown.

new underground accelerators have been proposed at a number of locations, namely: LNGS [14], the Canfranc laboratory in Spain [15], the planned DUSEL facility in the United States [16], Boulby mine in the United Kingdom [17], and Romania [18].

The present work is the third in a series [19,20] that aims to facilitate these efforts, by providing detailed background data on deep underground in-beam setups as a reference case. In the first article of the series, the laboratory background with no or only minor shielding was studied for high-purity germanium (HPGe) and bismuth germanate (BGO) γ -detectors, and it was shown that for $E_\gamma > 3$ MeV the laboratory γ -background at LUNA is typically three orders of magnitude lower than at the surface of the Earth [19]. The second article presented an ultra-low background (ULB) HPGe detector with a sophisticated passive shield at LUNA. For $E_\gamma \leq 3$ MeV, this in-beam setup [20] displayed a laboratory background close to that of dedicated, deep underground activity-counting setups [21].

Here, the effects of segmentation and of active shielding on the laboratory γ -background of a HPGe detector are studied. To this end, the background of a HPGe detector that has been used for a recent LUNA experiment [12] has been studied in detail. For some of the experiments, also a 5 cm thick lead shield has been added, allowing to investigate the combination of active and passive shielding. Finally, as an example of the potential applications of a composite HPGe detector deep underground, the weak branching ratio for the decay of the $E_p = 223$ keV resonance in the $^{24}\text{Mg}(p,\gamma)^{25}\text{Al}$ reaction to the ground state in ^{25}Al is redetermined.

2 Setup

For the experiment, a EURISYS Clover detector [22] has been used. This type of composite detector was selected

because it easily fits in the restricted space of an underground laboratory. It consists of four coaxial n-type HPGe detectors arranged like a four-leaf clover (fig. 1). The spacing between the crystals is only 0.2 mm, leading to a closely packed geometry. At the 1333 keV ^{60}Co line, a single crystal has a typical resolution of 2.2 keV and 20% relative efficiency.

The signals from the four crystals are split after the preamplifiers. One part is fed into four main amplifiers, and the signals are then digitized and recorded in self-triggered, histogramming mode. These four individual histograms were gainmatched and added channel by channel, to form just one histogram hereafter called "singles mode spectrum".

The second part is fed into an analog summing unit implementing the gain-matching and summing of the four signals. The analog sum signal is then passed to a fifth main amplifier and digitized. The signal can then be recorded either in free-running, self-triggered, mode (called hereafter "adback mode, free-running") or in anticoincidence with the signal from the BGO escape-suppression shield (called hereafter "adback mode, escape suppressed"). The virtual large detector formed by the adback mode has 122% relative efficiency, comparable to the HPGe detectors used for the previous background studies at LUNA [19,20].

The accidental suppression rate of the BGO escape-suppression shield was found to be 1%. The average number of hits per event was determined to be 1.1 for the laboratory background and 1.2 for the highest counting rate in-beam run, on the 278 keV resonance of the $^{14}\text{N}(p,\gamma)^{15}\text{O}$ reaction. The timing information from the individual crystals was not used. Due to the continuous character of the intensive ion beam at LUNA, no time correlation between ion beam and emitted γ -ray was possible.

In the present study, the Clover detector is always used in conjunction with a surrounding BGO scintillator. For the adback mode data, the BGO can act as a Compton suppression veto. For the singles mode data, the BGO was in effect only a passive shield. The detector was used in horizontal geometry, so that in adback mode, the BGO shield can act as a veto against penetrating muons passing the germanium detector volume.

3 Off-line experiments and results

For the underground experiments presented here, the Clover detector was placed deep underground in the LUNA facility [23] of LNGS. For a first set of measurements, it was mounted in horizontal geometry at the 45-2 beamline of the 400 kV LUNA2 accelerator, and no lead shielding was used. During the background measurement presented in the present section, the LUNA beam was off. This setup was used both for the off-line experiments without lead shield and for the in-beam experiment described below in sec. 4.

In a second part of the underground experiments, the detector was placed on the floor of the LUNA hall and

completely surrounded with a 5 cm thick shield of standard lead.

For comparison, measurements at the surface of the Earth were performed at FZD. The experimental hall has a ceiling equivalent to about 0.3 m water. No lead shielding was applied.

3.1 Laboratory background γ -lines

The main γ -lines present in the laboratory background (fig. 2) are identified as:

- 511 keV e^+e^- annihilation peak
- 570 and 1064 keV lines from ^{207}Bi . This isotope is a commonly observed contamination in BGO material, produced through the $^{206}\text{Pb}(p,\gamma)^{207}\text{Bi}$ reaction by cosmic rays. All BGO material shows some ^{207}Bi impurity, except in cases where the bismuth starting material has been obtained from lead-free ore.
- 609, 1120, and 2204 keV lines from the radon daughter ^{214}Bi . No anti-radon shielding was applied for the present study.
- 1173 and 1333 keV from some ^{60}Co contamination present in the BGO crystal.
- 1461 keV from ^{40}K present in the laboratory.
- 2615 keV from ^{208}Tl , in the Thorium chain. The background continuum caused by pileup of the laboratory background reaches up to 5200 keV, twice the energy of this highest γ -line (fig. 3).

Some further lines from radon daughters (^{228}Ac and ^{214}Bi) have also been observed but are neglected in the further discussion because they behave in an analogous manner to the three ^{214}Bi lines mentioned above.

The counting rates of the above mentioned γ -lines are summarized in table 1, for the two experiments at LUNA without and with lead shield, and for the reference case at the surface of the Earth. For comparison, the data from the previous study at the 45-1 beamline at LUNA using a single, large HPGe detector with 137% relative efficiency are also shown [20]. Those previous data [20] have been taken in several configurations. Here the previous data taken without shield and those taken with a sophisticated passive shield (25 cm selected lead with low ^{210}Pb content, 4 cm oxygen free high purity copper, anti-radon box) are shown for comparison.

As expected, the counting rates of the γ -lines from radioactive decays are hardly affected by going underground to LUNA because they are dominated by radioisotopes present in the walls of the laboratory or in the detector. When comparing the overground with the unshielded LUNA spectra, it is seen that the radon background (^{214}Bi) is a factor two lower at LUNA, due to the better ventilation of the LUNA site. The thorium background (^{208}Tl) is lower by a factor four, due to the different characteristics of the rock surrounding the LUNA site, as compared to the FZD hall. A similar effect is observed for the ^{40}K line and the e^+e^- annihilation peak. Only the γ -lines due to impurities contained in the BGO

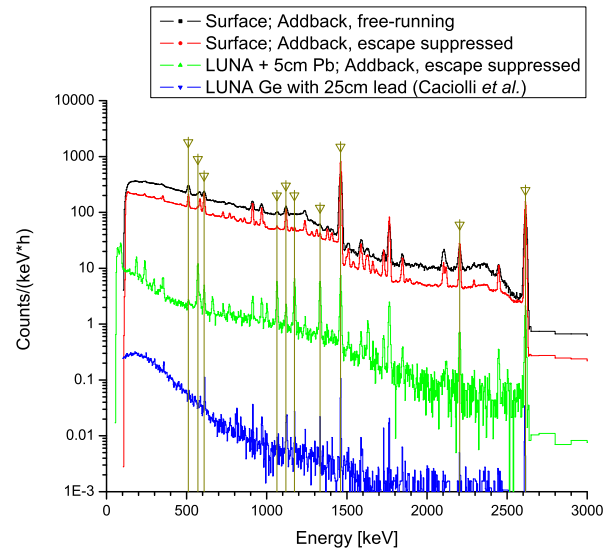


Fig. 2. Low energy part of the recorded laboratory γ -background spectra, compared with the previously described, strongly shielded setup at the 45-1 beamline at LUNA [20]. The lines marked with arrows are discussed in the text.

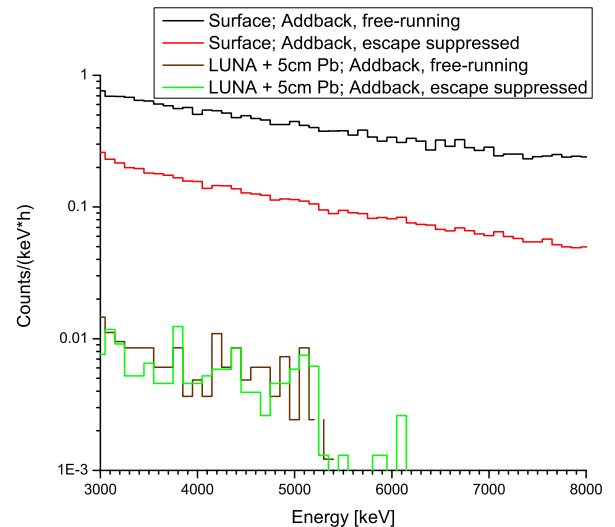


Fig. 3. High-energy part of the offline γ -spectra. At LUNA, the escape suppressed and the free-running spectra are indistinguishable in this energy range because the muon flux is so low that the remaining background is not dominated by muons any more, but by neutrons.

shield itself (^{207}Bi and ^{60}Co) do not change significantly between the different setups studied, as expected.

When comparing the unshielded and the shielded LUNA spectra, it is evident that already the present 5 cm lead shield leads to sizable reductions in the γ -line counting rates for all radioisotopes discussed above, except of course for the contaminations inherent to the BGO shield.

Table 1. Measured counting rates for radioactive decay lines, in counts per hour. Present data recorded with the Clover detector, are compared with the previous LUNA values [20] with a ULB detector and a passive shield consisting of 25 cm selected lead with low ^{210}Pb content, 4 cm oxygen free high purity copper, and an anti-radon box.

Source isotope E_γ [keV]		609	^{214}Bi 1120	2204	^{40}K 1461	^{208}Tl 2615	e^+e^- 511	^{207}Bi 570 1064	^{60}Co 1173 1333		
Clover, Earth's surface	singles	1013 \pm 52	509 \pm 26	182 \pm 10	6320 \pm 316	1163 \pm 58	1387 \pm 70	239 \pm 15	148 \pm 10	69 \pm 7	61 \pm 5
	adddback, free runn.	1405 \pm 81	750 \pm 47	318 \pm 19	10227 \pm 513	2046 \pm 104	1813 \pm 101	387 \pm 44	224 \pm 30	122 \pm 28	78 \pm 20
	adddback, esc. suppr.	1415 \pm 72	759 \pm 39	311 \pm 16	10065 \pm 503	1997 \pm 100	800 \pm 42	225 \pm 17	118 \pm 11	84 \pm 9	89 \pm 8
Clover at LUNA no shield	singles	532 \pm 27	258 \pm 13	90 \pm 5	861 \pm 43	284 \pm 14	306 \pm 16	244 \pm 13	149 \pm 8	54 \pm 3	52 \pm 3
	adddback, free runn.	750 \pm 38	398 \pm 20	150 \pm 8	1342 \pm 67	481 \pm 24	382 \pm 21	350 \pm 19	225 \pm 12	77 \pm 6	75 \pm 5
	adddback, esc. suppr.	717 \pm 36	380 \pm 19	147 \pm 8	1310 \pm 66	459 \pm 23	126 \pm 8	135 \pm 9	59 \pm 4	56 \pm 4	57 \pm 4
Clover at LUNA 5 cm Pb shield	singles	33 \pm 3	13 \pm 2	5.4 \pm 0.7	42 \pm 3	16.9 \pm 1.3	21 \pm 3	235 \pm 13	153 \pm 8	53 \pm 3	50 \pm 3
	adddback, free runn.	51 \pm 7	20 \pm 4	7.9 \pm 1.5	64 \pm 5	28.3 \pm 2.4	34 \pm 6	310 \pm 18	237 \pm 14	86 \pm 6	64 \pm 5
	adddback, esc. suppr.	30 \pm 3	15 \pm 2	7.6 \pm 0.9	71 \pm 4	21.0 \pm 1.6	5 \pm 3	98 \pm 6	47 \pm 3	59 \pm 4	58 \pm 4
ULB at LUNA [20]	no shield	3729 \pm 4	1278 \pm 3		4870 \pm 4	1325 \pm 2	762 \pm 4				
	25 cm Pb shield	0.30 \pm 0.04	0.15 \pm 0.02		0.42 \pm 0.03	0.12 \pm 0.02	0.09 \pm 0.04				

In order to estimate the possible effects of a full, state-of-the-art passive shielding on the present setup, it is useful to compare the present data with the data from the previous LUNA study [20] (table 1, last two lines). The unshielded starting point of the previous LUNA data is somewhat worse than for the present work, because in the present detector the BGO also acts as passive shield due to its high γ -attenuation coefficient. However, the factors of improvement seen when comparing the last two lines of table 1 show which low levels of background can in principle be reached using a full passive shield like in Ref. [20].

3.2 Laboratory background continuum

For in-beam experiments, the γ -ray continuum observed in regions outside of the laboratory background lines is of paramount importance. For reaction Q -values above 3 MeV, in principle also γ -rays of energies above 3 MeV can be emitted, in a region where there are no γ -lines from radioisotopes. Furthermore, for primary in-beam γ -rays the resolution is in many cases not limited by the detector, but by the effective target thickness, making the γ -lines rather wide, adding further importance to obtaining a low continuum in γ -detectors.

At the surface of the Earth, the two main sources of the γ -continuum are the Compton continuum of γ -rays and the energy loss or stopping of cosmic-ray induced particles like muons. An escape-suppression veto detector like the present BGO shield can strongly reduce both effects. In addition, placing the setup deep underground, thus reducing the muon flux, should lead to a further reduction of the γ -continuum, both for $E_\gamma < 3$ MeV [20] and $E_\gamma \geq 3$ MeV [19]. For example, a previous Monte Carlo simulation [24] predicts an overall factor of three reduction for $E_\gamma < 3$ MeV, when comparing overground spectra with a shallow underground facility at a depth of 30 m water equivalent.

In order to verify these expectations, the continuum counting rate has been determined for some regions of interest (ROI's) that are important for nuclear reactions that might conceivably be studied in underground accelerator experiments (table 2). These reactions and the as-

trophysical motivation driving their study have been discussed previously [20].

For $E_\gamma < 3$ MeV, it is clear from table 2 that the present detector, which has some internal contamination and is at maximum shielded with 5 cm lead, cannot reach the background suppression factors of the previous LUNA study [20] with its much better shield (table 2, last line).

For $E_\gamma \geq 3$ MeV overground, it is found from the present data that the escape suppression reduces the continuum counting rate by a factor 11. This reduction is comparable to the factor 10–50 reported for $E_\gamma = 7$ –11 MeV from a previous overground experiment using a HPGe detector shielded by a NaI escape-suppression shield [25].

By placing the detector deep underground at LUNA, in the same energy region the continuum counting rate is improved by an additional factor of 30 when compared with the overground, escape suppressed run (fig. 3). For $2.6 \text{ MeV} < E_\gamma < 5.2 \text{ MeV}$ (two times the energy of the ^{208}Tl γ -ray), the LUNA spectra are dominated by pileup from natural radionuclides. This background is not affected by the BGO veto detector, but it can instead be rejected using suitable electronic pileup rejection logic. However, for LUNA-type experiments such circuits may lead to increased uncertainty, because at low counting rate it is not easy to properly adjust them. Therefore, no pileup rejection circuit is used here.

At LUNA, the escape suppression does not produce any further effect for $E_\gamma > 5.2$ MeV, as expected when muons make a negligible contribution to the background (table 2). Similarly, the 5 cm lead shield does not lead to a further reduction in counting rate at LUNA, which can be explained by the fact that radioisotopes don't contribute significantly to the background for $E_\gamma \geq 5.2$ MeV. The remaining background values shown for the present detector are consistent with the previous data for a similar germanium detector with 5 cm lead shield at LUNA [19]. This background level is explained with neutron capture from the remaining flux of thermal and high-energetic neutrons present in LNGS [26].

Table 2. Continuum counting rate in counts/(keV hour) for several regions of interest relevant to radiative capture reactions.

Reaction γ -ray ROI [keV]		$^{12}\text{C}(^{12}\text{C},\text{p})^{23}\text{Na}$ 425-455	$^2\text{H}(\alpha,\gamma)^6\text{Li}$ 1545-1575	$^3\text{He}(\alpha,\gamma)^7\text{Be}$ 1738-1753	$^{12}\text{C}(\text{p},\gamma)^{13}\text{N}$ 2004-2034	$^{24}\text{Mg}(\text{p},\gamma)^{25}\text{Al}$ 2470-2500	$^{14}\text{N}(\text{p},\gamma)^{15}\text{O}$ 6000-8000
Clover, Earth's surface	singles	259.4 ± 0.2	16.02 ± 0.06	10.79 ± 0.07	8.48 ± 0.04	3.81 ± 0.03	$(128.9 \pm 0.8) \times 10^{-3}$
	addback, free running	317.3 ± 0.8	22.64 ± 0.21	15.84 ± 0.25	12.67 ± 0.16	6.33 ± 0.05	$(205.6 \pm 1.1) \times 10^{-3}$
	addback, escape suppressed	162.2 ± 0.2	11.48 ± 0.05	8.36 ± 0.06	5.75 ± 0.04	4.07 ± 0.03	$(19.2 \pm 0.4) \times 10^{-3}$
Clover at LUNA no shield	singles	64.57 ± 0.14	5.29 ± 0.04	3.09 ± 0.04	2.17 ± 0.02	0.72 ± 0.01	$(0.17 \pm 0.03) \times 10^{-3}$
	addback, free running	77.64 ± 0.18	7.52 ± 0.06	4.98 ± 0.07	3.13 ± 0.04	1.27 ± 0.02	$(0.15 \pm 0.04) \times 10^{-3}$
	addback, escape suppressed	30.52 ± 0.14	3.12 ± 0.04	2.71 ± 0.06	1.17 ± 0.03	0.73 ± 0.02	$(0.18 \pm 0.05) \times 10^{-3}$
Clover at LUNA 5 cm Pb shield	singles	6.35 ± 0.11	0.40 ± 0.03	0.19 ± 0.03	0.130 ± 0.015	0.06 ± 0.01	$(0.28 \pm 0.12) \times 10^{-3}$
	addback, free running	6.95 ± 0.17	0.57 ± 0.05	0.34 ± 0.05	0.21 ± 0.03	0.11 ± 0.02	$< 0.11 \times 10^{-3}$
	addback, escape suppressed	2.47 ± 0.07	0.26 ± 0.02	0.16 ± 0.03	0.076 ± 0.013	0.05 ± 0.01	$(0.29 \pm 0.13) \times 10^{-3}$
HPGe at LUNA ULB at LUNA	5 cm Pb shield [19] 25 cm Pb shield [20]	0.072 ± 0.002	0.0015 ± 0.0003	0.0011 ± 0.0003	0.0009 ± 0.0003		$< 0.1 \times 10^{-3}$

3.3 Addback factor

For the present data on the laboratory background lines (table 1), the addback factor [22]

$$\text{ABF} \stackrel{!}{=} \frac{C_{\text{addback, free-running}}}{C_{\text{singles}}} \quad (1)$$

has been calculated. Here, $C_{\text{addback, free-running}}$ is the counting rate in addback mode, free-running, and C_{singles} is the singles mode counting rate. The same has been done also for some γ -lines emitted in the $^{14}\text{N}(\text{p},\gamma)^{15}\text{O}$ reaction studied with the present detector and setup.

The data points all follow the same general curve, despite the very different points of emission of the various γ -rays: outside contaminations, radioactivity in the BGO shield, or decays in the air close to the detector (fig. 4). The present high-energy data points lie close to the previous fitted curve [27], confirming that the slope is somewhat higher than initially expected [22].

4 Decay of the $E_p = 223$ keV resonance in the $^{24}\text{Mg}(\text{p},\gamma)^{25}\text{Al}$ reaction as an example

4.1 General considerations

When studying the γ -decay of an excited nuclear state (e.g. the $E_x = 2485$ keV state in ^{25}Al , fig. 5), usually not only direct decay to the ground state of the nucleus, but also cascade decays via intermediate states are observed. Therefore in the observed γ -ray spectrum the signal from the transition to the ground state can be obscured by an artefact that appears at exactly the same energy, due to the true coincidence summing effect. This effect is usually corrected for in an analytic manner. However, in cases where the summing-in effect is large when compared to the true signal, such a correction can lead to considerable systematic uncertainty.

The magnitude of the summing-in correction is directly proportional to the absolute γ -detection efficiency. Therefore, one possible approach to limit summing-in is to move the detector to a larger distance, sacrificing efficiency and angular coverage. However, in low-energy nuclear astrophysics experiments, usually the γ -ray emission rate is

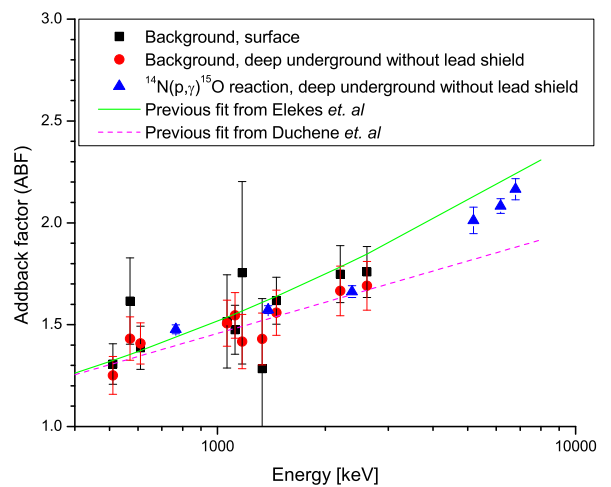


Fig. 4. Symbols, addback factor ABF calculated according to eq. 1 for γ -lines from the laboratory background (table 1): Squares, Earth's surface; circles, deep underground without lead shield. Triangles, ABF for γ -lines from the the $^{14}\text{N}(\text{p},\gamma)^{15}\text{O}$ reaction. Solid (dashed) line, previous fitted curves from Ref. [27] (from Ref. [22]).

low and their angular distribution not very well known. Solving the summing problem in this way therefore worsens two other problems, the low statistics and the dependence on the angular distribution. Therefore in the past at LUNA this approach could only be used for data on strong resonances [29].

An alternative approach is to use a composite detector. For the present case of four independent crystals, the summing-in effect is reduced by 4-ABF (i.e. four times the addback factor, ABF), while the γ -efficiency is only reduced by ABF. The angular coverage even remains unchanged. As an additional piece of information, the addback data can also be analyzed, and the comparison of singles and addback mode data can serve as a check on the analytical summing correction for the addback data.

A further advantage of using a composite detector, the much lower Doppler correction for each single crystal, has only limited importance for low-energy nuclear astro-

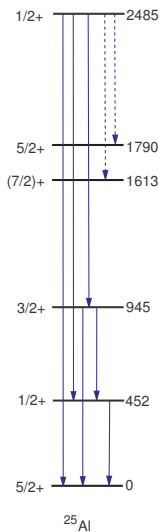


Fig. 5. Level scheme of ^{25}Al [28]. Full arrows, γ -transitions observed in the present experiment. Dashed arrows, γ -transitions where new upper limits have been derived.

physics studies. For Gamow peak energies of a few ten keV, the typical velocity of the recoil nuclei is lower than 1%, and the typical Doppler correction for LUNA-type experiments is of the same order as the energy resolution of the HPGe detector.

4.2 Branching ratio determination

In order to illustrate these considerations, the weak ($\approx 3\%$) ground state branching of the $E_p = 223$ keV resonance in the $^{24}\text{Mg}(p,\gamma)^{25}\text{Al}$ reaction (corresponding to the $E_x = 2485.3$ keV level in ^{25}Al , fig. 5) is redetermined here. This reaction plays a role in the hydrogen-burning MgAl chain [30].

For the experiment, a magnesium oxide target of natural isotopic composition (79% ^{24}Mg) was used. The Clover detector was placed at 55° with respect to the ion beam, with its front face at 9.5 cm distance from the target. The γ -detection efficiency is well-known from another experiment in exactly the same geometry [12], and the slope from 695 keV to 2485 keV is known to 1.0%. By scanning the target profile, an energy near the center of the target was selected. Then a spectrum was recorded on top of the resonance (fig. 6). With a strength of (12.7 ± 0.9) meV [31], the resonance is sufficiently intensive that off-resonance capture can be neglected for the present purposes. The laboratory background is comparable in intensity to the in-beam lines, as is apparent from the similar yield of the in-beam line at 2485 keV and the laboratory background line at 2615 keV (fig. 6). However, the background γ -lines lie at different energies, so the background does not limit the statistics of the 2485 keV ground state line (table 2).

The branching ratios for the decay of the resonance have then been determined (table 3). For the ground state capture line, the calculated summing-in correction was

Table 3. Branching ratios, in %, for the decay of the $E_p = 223$ keV resonance in the $^{24}\text{Mg}(p,\gamma)^{25}\text{Al}$ reaction. Where applicable, upper limits are given for 90% confidence level.

Decay	Literature [31]	Present work	
		addback	singles
$2485, \frac{1}{2}^+ \rightarrow 0, \frac{5}{2}^+$	2.7 ± 0.3	2.6 ± 0.2	2.69 ± 0.08
$\rightarrow 452, \frac{1}{2}^+$	81.7 ± 3.4	81.8 ± 1.2	81.6 ± 1.1
$\rightarrow 945, \frac{3}{2}^+$	15.6 ± 1.1	15.6 ± 0.5	15.7 ± 0.6
$\rightarrow 1613, \frac{7}{2}^+$	< 0.8	< 0.3	< 0.3
$\rightarrow 1790, \frac{5}{2}^+$	< 0.8	< 0.3	< 0.3

37% (7%) for the addback (singles) mode data, respectively. Assuming a conservative 20% relative uncertainty for all the summing-in and summing-out corrections, due to the summing correction there is 0.19% (0.04%) absolute uncertainty in the ground state branching for addback (singles) mode. For the addback case, this dominates the total uncertainty of 0.2%. The fact that the branching ratio as determined in the addback mode agrees with the singles mode data confirms that the summing-in correction is accurate.

For the primary γ -ray from the major transition, capture to the 452 keV first excited state, 3% (0.7%) summing-out correction was taken into account for addback (singles) mode. For the primary γ -ray from capture to the 945 keV state, 5% (1.0%) summing-out correction was taken into account, and again the addback and singles data are in agreement.

The newly determined branching ratios are in agreement with the literature data [31] but more precise. No significant branching is expected for the M3 transition to the $\frac{7}{2}^+$ level at 1613 keV and the E2 transition to the $\frac{5}{2}^+$ level at 1790 keV. The present data bear out this expectation, giving new experimental upper limits for these two transitions (table 3). The values obtained in singles mode are recommended for future compilations [28].

In the previous measurement [31], a large volume (140%) HPGe detector had been placed at 55° with respect to the beam direction, at 5.9 cm distance to the target. Based on these numbers, we estimate that in singles mode, the present summing-in correction is about a factor 9 lower than in Ref. [31], justifying the present lower uncertainty.

Another example studied recently is the $^{14}\text{N}(p,\gamma)^{15}\text{O}$ reaction, which controls the rate of the hydrogen-burning CNO cycle [30]. Due to the complicated interference pattern of several components in the R-matrix framework, the rather weak capture to the ground state in ^{15}O dominates the uncertainty of the total extrapolated $^{14}\text{N}(p,\gamma)^{15}\text{O}$ cross section at energies corresponding to solar hydrogen burning. The study of this transition is affected by summing-in corrections, and with the present detector and setup recently an experiment with greatly reduced summing corrections has been performed [12].

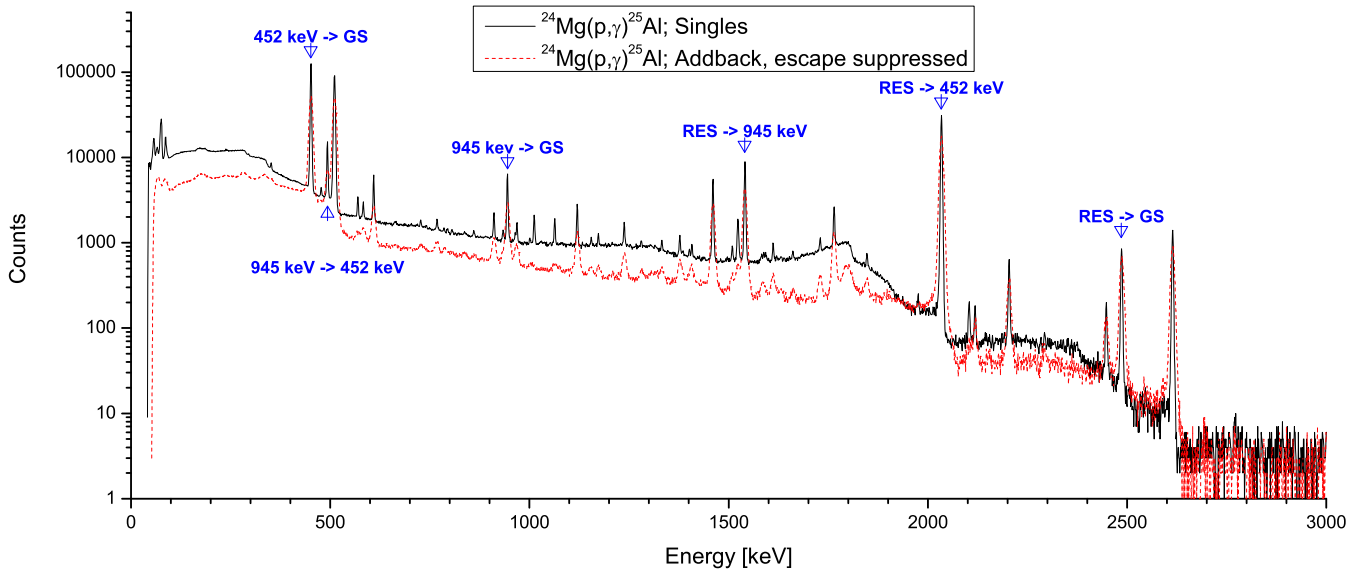


Fig. 6. In-beam γ -spectrum on the top of the $E_p = 223$ keV resonance in the $^{24}\text{Mg}(p,\gamma)^{25}\text{Al}$. Black full (red dashed) line, singles mode (addback mode, escape suppressed) data. The most important transitions are marked.

5 Discussion and outlook

A Clover-BGO detector system for nuclear astrophysics experiments has been used deep underground at LUNA. The laboratory background of one and the same detector has been studied in detail at LUNA and in an overground laboratory for reference. It is found that by going deep underground, the γ -continuum background counting rate can be reduced much more than by simply applying a cosmic-ray veto.

In free-running mode, the background characteristics of the present detector at LUNA are comparable to single detectors of similar size at LUNA, when a shielding similar to the present one is applied. The escape suppression was shown to further reduce the γ -continuum background counting rate.

In order to illustrate the applications of a composite, escape-suppressed detector in underground nuclear astrophysics, the weak ground state branching of the $E_p = 223$ keV resonance in the $^{24}\text{Mg}(p,\gamma)^{25}\text{Al}$ reaction has been determined with improved precision.

A further step in studying the potential of a composite, escape-suppressed detector in a deep underground accelerator laboratory such as LUNA would be to construct an ultra-low background composite detector with a long neck to accommodate a full lead and copper shield.

Acknowledgments

The present work has been supported by INFN and in part by the EU (ILIAS-TA RII3-CT-2004-506222), OTKA (T49245 and K68801), and DFG (Ro 429/41). T.S. acknowledges a Herbert Quandt fellowship at Technical University Dresden.

References

1. M. Asplund, N. Grevesse, and A. Jacques Sauval, *Nucl. Phys. A* **777**, 1 (2006).
2. C. Peña-Garay and A. Serenelli, ArXiv e-prints (2008), 0811.2424.
3. A. M. Serenelli, S. Basu, J. W. Ferguson, and M. Asplund, *Astrophys. J. Lett.* **705**, L123 (2009), 0909.2668.
4. U. Greife *et al.*, *Nucl. Inst. Meth. A* **350**, 327 (1994).
5. A. Formicola *et al.*, *Nucl. Inst. Meth. A* **507**, 609 (2003).
6. R. Bonetti *et al.*, *Phys. Rev. Lett.* **82**, 5205 (1999).
7. C. Casella *et al.*, *Nucl. Phys. A* **706**, 203 (2002).
8. A. Formicola *et al.*, *Phys. Lett. B* **591**, 61 (2004).
9. A. Lemut *et al.*, *Phys. Lett. B* **634**, 483 (2006).
10. D. Bemmerer *et al.*, *Phys. Rev. Lett.* **97**, 122502 (2006).
11. F. Confortola *et al.*, *Phys. Rev. C* **75**, 065803 (2007).
12. M. Marta *et al.*, *Phys. Rev. C* **78**, 022802(R) (2008).
13. D. Bemmerer *et al.*, *J. Phys. G* **36**, 045202 (2009).
14. Nuclear Physics European Collaboration Committee (NuPECC), Roadmap 2005, available at http://www.nupecc.org/pub/NuPECC_Roadmap.pdf.
15. Workshop on Nuclear Astrophysics Opportunities at the Underground Laboratory in Canfranc, Barcelona 19-20 February 2009, <http://www.fnuc.es/workshop/canfranc.html>.
16. DOE/NSF Nuclear Science Advisory Committee, arXiv:0809.3137.
17. F. Strieder, *J. Phys. G* **35**, 014009 (2008).
18. C. Bordeanu *et al.*, *J. Phys. G* **35**, 014011 (2008).
19. D. Bemmerer *et al.*, *Eur. Phys. J. A* **24**, 313 (2005).
20. A. Cacioli *et al.*, *Eur. Phys. J. A* **39**, 179 (2009).
21. M. Laubenstein *et al.*, *Appl. Radiat. Isot.* **61**, 167 (2004).
22. G. Duchêne *et al.*, *Nucl. Inst. Meth. A* **432**, 90 (1999).
23. H. Costantini *et al.*, *Rep. Prog. Phys.* **72**, 086301 (2009).
24. P. Vojtyla and P. P. Povinec, *Radioactivity in the Environment* **8**, 529 (2006).
25. G. Müller *et al.*, *Nucl. Inst. Meth. A* **295**, 133 (1990).

26. P. Belli *et al.*, *Nuovo Cimento A* **101**, 959 (1989).
27. Z. Elekes *et al.*, *Nucl. Inst. Meth. A* **503**, 580 (2003).
28. R. B. Firestone, *Nucl. Data Sheets* **110**, 1691 (2009).
29. G. Imbriani *et al.*, *Eur. Phys. J. A* **25**, 455 (2005).
30. C. Iliadis, *Nuclear Physics of Stars* (Wiley-VCH, 2007).
31. D. C. Powell *et al.*, *Nucl. Phys. A* **660**, 349 (1999).